Title: An actionable map of arm and hand muscle responses to electrical stimulation of the dorsal cervical spinal cord in humans

James R. McIntosh[a, d], Evan. F. Joiner[b], Jacob L. Goldberg[d], Lynda M. Murray[h, i], Bushra Yasin[a, d], Anil Mendiratta[c], Steven C. Karceski[e], Earl Thuet[f], Oleg Modik[e], Evgeny Shelkov[e], Christopher Mandigo[b,f], K. Daniel Riew[a, d, f], Noam Y. Harel[g, h, i], Michael S. Virk[d, f, *], Jason B. Carmel[a, c, d, *]

[a]Dept. of Orthopedic Surgery, [b]Dept. of Neurological Surgery, [c]Dept. of Neurology, Columbia University, 650 W. 168th St, New York, NY, 10032, USA

[d]Dept. of Neurological Surgery., [e]Dept. of Neurology, NewYork-Presbyterian/Weill Cornell Medicine, 1300 York Ave, New York, NY 10065

[f]New York Presbyterian, The Och Spine Hospital, 5141 Broadway, New York, NY 10034

[g]Departments of Neurol., [h]Rehabil. and Human Performance, Icahn Sch. of Med. at Mount Sinai, One Gustave L. Levy Place, New York, NY 10029

[i]James J. Peters VA Med. Ctr., 130 West Kingsbridge Road, Bronx, NY 10468

*J. B. Carmel and M. S. Virk should be considered joint senior authors.

Correspondence should be addressed to J. B. Carmel (jason.carmel@columbia.edu) or J. R. McIntosh (j.mcintsoh@columbia.edu)

Abstract

While epidural stimulation of the lumbar spinal cord has emerged as a powerful modality for recovery of movement, how it should be targeted to the cervical spinal cord to activate arm and hand muscles is not well-understood, particularly in humans. We sought to map muscle responses to posterior epidural cervical spinal cord stimulation in humans. We hypothesized that lateral stimulation over the dorsal root entry zone would be most effective, and responses would be strongest in the muscles innervated by the stimulated segment. Eighteen people undergoing clinically indicated cervical spine surgery were enrolled. During surgery, stimulation was performed in midline and lateral positions at multiple exposed segments; eight arm and three leg muscles were recorded on each side of the body. Across all segments and muscles tested, lateral stimulation produced stronger muscle responses than midline. These stronger responses were due to a combination of a decreased response threshold and steeper recruitment slope. Muscles innervated at a cervical segment had the largest responses from stimulation at that segment, but responses were also observed in muscles innervated at other cervical segments and in leg muscles. The cervical responses were clustered in rostral (C4-C6) and caudal (C7-T1) cervical segments. Strong responses to lateral stimulation are likely due to the proximity of stimulation to afferent axons. Small changes in responses to stimulation of adjacent cervical segments argues for local circuit integration, and distant muscle responses suggest activation of long propriospinal connections. This map can help guide cervical stimulation to improve arm and hand function.

Significance Statement

Epidural stimulation of the human lumbar spinal cord for movement recovery after injury has been guided by a map of muscle responses to stimulation, but no such map exists for the human cervical spinal cord. A map of muscle responses to cervical epidural stimulation during clinically indicated surgery revealed a much stronger effect of changes in midline versus lateral stimulation compared with stimulation at different cervical segments. In addition, muscle responses were highly correlated between each segment within the upper cervical enlargement (C4-C6) and within the lower cervical enlargement (C7-T1), but these regions were not as similar to each other. Thus, a map of cervical spinal cord stimulation reveals its internal organization and may help guide therapy.

1 Introduction

Epidural stimulation has emerged as a way to modify spinal cord circuits for movement recovery (Carhart et al. 2004; Wagner et al. 2018; Angeli et al. 2018; Gill et al. 2018). These studies largely targeted the lumbar spinal cord, with its relatively well-defined central pattern generator (Dimitrijevic, Gerasimenko, and Pinter 1998; Danner et al. 2015). In contrast, the circuit-level logic of where and how to stimulate the cervical spinal cord is not as well known. Since hand function is the top priority of people with cervical spinal cord injury (SCI) (Anderson 2004; Snoek et al. 2004), interventions are under development to target the cervical spinal cord (Lu et al. 2016; Freyvert et al. 2018; Inanici et al. 2021; Kumru et al. 2021; Pal et al. 2021). Effective stimulation of the cervical spinal cord may be more difficult than for the lumbosacral spinal cord given its large behavioral repertoire, and poorly understood intrinsic programs (Dietz 2002). The current study used electrical stimulation during clinically indicated cervical spine surgery to improve understanding of cervical spinal cord circuits.

Some of the insights learned from lumbar epidural stimulation apply to the cervical spinal cord. Stimulation of the dorsal spinal cord at low intensity evokes muscle responses via large-diameter afferents and not by direct activation of motoneurons (Hofstoetter et al. 2018; Wu et al. 2020). Electrical stimulation of afferents activates motoneurons through circuits involved in reflexes (Renshaw 1940; Lloyd 1943). This mechanism has been corroborated by mathematical modeling of current flow (Rattay, Minassian, and Dimitrijevic 2000; Capogrosso et al. 2013; Greiner et

al. 2021) as well as in inactivation studies (Pal et al. 2021). Consistent with this model, we have shown that stimulating near the dorsal root entry zone is more effective than stimulating at midline in rats (Mishra et al. 2017).

Dorsal epidural stimulation of a cervical segment activates muscles innervated at that segment with spread to others. Muscle responses to epidural stimulation of the cervical spinal cord (Sharpe and Jackson 2014; Greiner et al. 2021) broadly correspond to the distribution of motor pools throughout the cervical cord (Jenny and Inukai 1983; Chiken, Hatanaka, and Tokuno 2001). The spread of responses beyond the stimulated segment may be due to spread of afferents (Tubbs et al. 2009; Atik et al. 2019), or variability in motoneuron to muscle connections (Bollini and Wikinski 2006). For example, with the exception of the separation between the biceps and triceps, Greiner et al. (Greiner et al. 2021) observed a considerable overlap in the activated muscles at each cervical spinal segment in macaque monkeys. When stimulating dorsally in humans this breadth of activation of individual muscles across multiple segments is present, however, some additional divergence has also been found (Schirmer et al. 2011), with the most extreme observation being of leg muscle activation to dorsal epidural cervical stimulation (Dimitrijevic et al. 1980). In fact, leg muscle activation has also been observed in transcutaneous dorsal cervical stimulation (Sabbahi et al. 2014).

These data led us to hypothesize that epidural stimulation of each cervical segment would activate large diameter afferents, causing strongest contraction of muscles innervated at that segment when stimulating laterally near the dorsal root entry zone. The detailed predicted results are shown in Fig. 1b, with larger circles representing larger MEPs provoked by stimulation at that location in biceps (purple) or triceps (green). Similar to our studies in rats (Mishra et al. 2017), we predicted that lateral stimulation of the spinal cord (lighter shade), would be more effective than midline stimulation (darker). The strongest responses would be observed at the segment of innervation (e.g. C5 and C6 for biceps (Yonemura et al. 2004) and C7 for triceps) with spread from there to adjacent segments. Taken together, we expected that for most segments there would be a larger change in motor evoked potentials when comparing midline to lateral stimulation within each segment than when comparing rostral-caudal cervical segments.

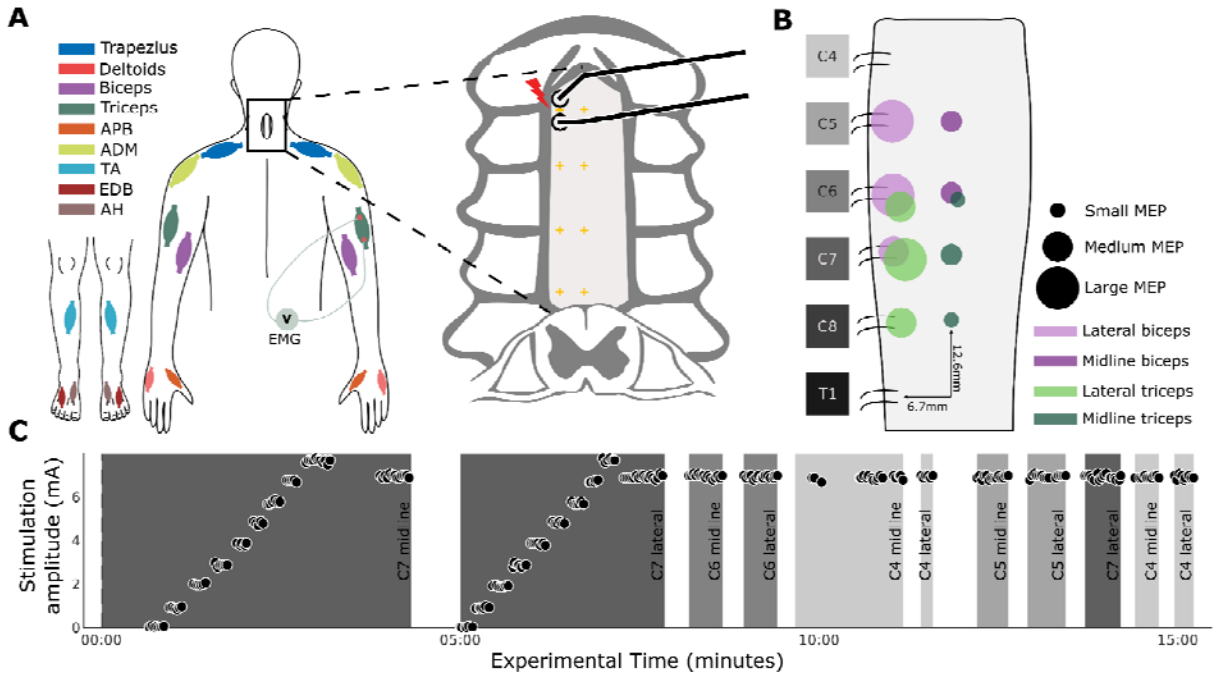

Figure 1. Epidural stimulation experiment during posterior cervical spine surgery. **(A)** Prior to surgery, each patient was rotated prone onto a Jackson table after his or her head was placed in Gardner-Wells tongs. The head was suspended with 15 pounds of neutral traction. Arms were tucked to the side with thumbs facing towards the floor, and all pressure points were padded. Once the dura was exposed by laminectomy, a handheld or catheter electrode was used to stimulate at multiple segmental locations in either the lateral or midline position. Colors correspond to different recorded muscles (see legend). **(B)** Hypothesized responses to epidural stimulation of the cervical cord for a subselection of muscles. Previous work had indicated that muscle activation for dorsal cervical stimulation is primarily mediated by afferents. This generated the following hypotheses: 1) Lateral stimulation over the dorsal root entry zone was expected to be more effective than stimulation over the midline (large circles, representing high activation are lateral, while smaller circles are placed along the midline). 2) Muscle activation was expected to be relatively localized in the rostral caudal direction, however some spread of this activation was expected due to tight interconnection of sensory circuits throughout the cervical cord (circles for a given muscle are spread out in the rostral-caudal orientation). **(C)** Example sequence of the 15 minute experiment. Initially, the electrode was placed along the midline, over the dura at a segment aligned with the expected location of the root entry (C7 midline for this experiment). The stimulation intensity was ramped up with two purposes: 1) in search of the threshold of a target muscle. 2) To gather threshold information for multiple muscles in a single sweep. Once the threshold was found stimulation was performed at 1.2× that value (referred to as 'fixed intensity'). The ramp procedure followed by the fixed intensity was then repeated laterally to enable a midline-lateral comparison. The experiment proceeded with fixed intensity stimulation only, due to the time constraints of the surgery. Stimulation was performed at multiple segments at both midline and lateral locations.

2 Materials and methods

2.1 Experimental design

People undergoing clinically indicated spine surgery had epidural electrical stimulation of the exposed segments of the cervical spinal cord and recording of motor evoked potentials (MEPs) from arm and leg muscles (Fig. 1A). This dedicated period of intraoperative physiology testing lasted for a maximum of 15 minutes. To test the prediction that lateral stimulation would be more effective than midline, stimulation at each of these sites was compared (Fig. 1B). To

test the prediction that stimulation at one cervical segment would produce the largest responses in muscles innervated at that segment, stimulation at multiple cervical roots was performed. To test the prediction that movement in midline-lateral direction would produce larger changes than in the rostro-caudal direction, the size of MEP change over change in distance was computed for each direction (see Methods section "Comparison of responses at different cervical segments"). A representative experiment is shown in Fig. 1C. The primary outcome was the size of the MEP, and the secondary outcomes were the threshold and slope of the recruitment curve with increasing stimulus intensity.

2.2 Participants

Participants were adult patients with cervical spondylotic myelopathy or multilevel foraminal stenosis requiring surgical treatment (Table 1, extended Table 1-1). Patients were enrolled from the clinical practices of the spine surgeons participating in the study. The study protocol was reviewed and approved by the institutional review boards of the two study sites, Weill Cornell Medical Center and Columbia University Irving Medical Center. Patients with stimulation devices in the neck or chest (e.g. vagal nerve stimulation, cardiac patients with pacemakers) were excluded. Informed consent for participation in the study was obtained prior to surgery. Participants underwent standard of care preoperative clinical assessments. The modified Japanese Orthopaedic Association (mJOA) scores were used to assess the severity of myelopathy. Surgical time was not extended by the experimental procedure for longer than 15 minutes to limit the surgical and anesthetic risk of increased intraoperative time (Brendler 1968). These experiments were powered with effect size based on comparisons of midline and lateral stimulation in the rat (Mishra et al. 2017). Conservatively assuming a reduced effect size by 50% compared to the rat experiments (Cohen's $d = 0.97$ versus 1.94), the analysis indicated that to achieve 90% power using a Wilcoxon signed-rank test ($\alpha = 0.05$) would require 14 participants.

2.3 Electrophysiology

This study was conducted with the standard intraoperative neuromonitoring montage and by the neurophysiology staff used during all cervical spine surgeries performed at our institutions. After anesthesia induction, only total intravenous anesthesia was used. No anesthetic adjustments were made during the 15 minutes dedicated to the experiment. Recording and stimulation were performed with Cadwell Elite/Pro, Cadwell IOMAX (Cadwell Inc.) or XLTEK

Protektor32 (Natus Medical Inc.) intraoperative monitoring systems. The device chosen for a particular experiment was dependent on the study site and availability (see extended Table 1-1). The experimental procedure began once the dorsal dura was exposed and the epidural stimulation electrode was placed. Muscles were chosen for electromyogram (EMG) per standard of care (Fig. 1A). EMG responses were recorded with percutaneous needles at a sampling rate between 6kHz and 10.4kHz and bandpass filtered between 10Hz and 2000Hz. Epidural spinal cord stimulation was performed primarily in trains of 3 pulses (see extended Table 1-1) with a hand-held double ball tip probe (2.3mm diameter contacts, 10mm spacing); a catheter electrode was also used in 5 cases, as described below. Three-pulse stimulation was used to reduce the intensity necessary to evoke an MEP in order to reduce current spread (Moritz et al. 2007) In each case, the electrodes were oriented in the rostro-caudal direction (Fig. 1A, inset) with the cathode caudal. At each testing site, stimulation was delivered every 2 seconds, a frequency that we determined does not alter responses (data not shown).

2.3.1 Confirmation of electrode position over the dorsal root entry zone

When placed laterally, electrodes were positioned straddling the expected location of the dorsal root entry zone in a rostral-caudal orientation as identified by bony anatomical landmarks. Electrode placement based on anatomical landmarks was subsequently confirmed to be over the dorsal root entry zone via image reconstruction and coregistration between preoperative MRI and intraoperative CT scans performed in one participant. Clinically indicated intraoperative-CT (Airo, Striker Inc.) and pre-operative MRI (T2-weighted, Siemens) were gathered for this participant. During the course of the experiment, the location of the C7 root entry was inferred based on the bony landmarks of the spine. After placing the electrode at that site an intraoperative photograph was taken (Fig. 2A). The location of the electrode was then translated to a location in the CT based on instrumentation inserted during surgery (Fig. 2B). The CT and MRI images were then co-registered by performing a non-linear registration with the "Curvature Correction" software (Brainlab AG) to account for the different curvature of the spine in prone (operative) and supine (preoperative) participant position (Fig. 2C). The transformation generated in the registration was then also applied to the location of the electrode in the CT and shown in the MRI (Fig. 2D). The electrode position in the MRI appeared over the C7 root entry, in the intended location.

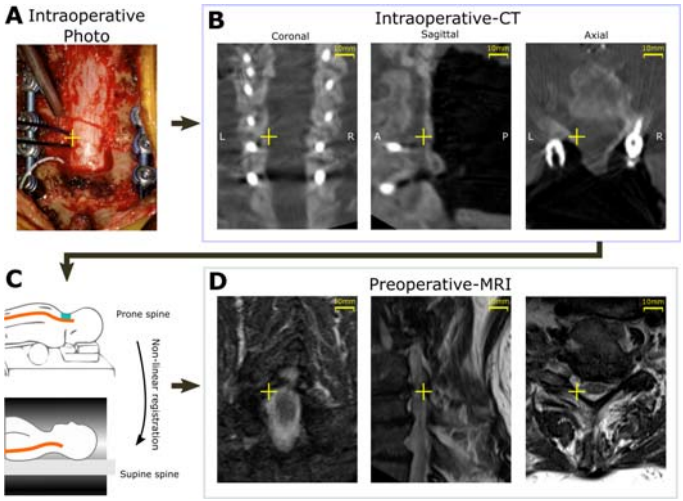

Figure 2. Validation of stimulation location relative to dorsal root entry zones. (A) A photograph was used to identify the position of electrodes relative to instrumentation. **(B)** This location was translated to a CT scan used to confirm implant location (yellow crosshatch). **(C)** CT and MRI images were co-registered by performing a non-linear segmental registration (Brainlab AG) to account for differences in spinal alignment found in prone (operative) and supine (preoperative) positions. **(D)** Electrode position in MRI near targeted C7 root verified location.

2.3.2 Comparison of midline versus lateral stimulation

Within each cervical segment, midline stimulation was compared with lateral stimulation. Midline electrode placement was determined by visual estimation and confirmed with measurement from the bony landmarks on either side. Electrodes were allowed to dimple the surface of the dura to one-third to one-half the depth of the ball tip. . Prior to the start of the experiment, we designated the lateral stimulation to be performed on the left or right to match each participant's less impaired side based on clinical signs, symptoms and MRI; this was done to minimize interaction of neurological deficits on electrophysiological responses.

Stimulation sites and intensity. An example of one experiment is shown in Fig. 1C. To begin each experiment, the stimulation electrode was placed on midline at the most caudal segment exposed during surgery. Stimulation intensity was incrementally increased from 0 to 8mA in order to assess the activation threshold and estimate the subsequent recruitment curve (minimum 10s per stimulation intensity; first panel Fig. 1C). Threshold was defined as the lowest stimulation intensity to produce an MEP in the most responsive muscle. The threshold of this muscle (Extended

Table 1-1) was used to set the fixed stimulus intensity (120% of threshold) for 30 seconds of stimulation at other segments. The experiments proceeded by repeating the stimulation intensity ramp and fixed intensity stimulation at the equivalent lateral site (second panel of Fig. 1C).

2.3.3 Comparison of responses at different cervical segments

MEPs at multiple segments were compared using the fixed intensity, which was repeated at more rostral sites (third panel onwards of Fig. 1C). This stimulation protocol was applied in all experiments. Additional experimental conditions were tested in a total of 7 participants (see extended Table 1-1) using single pulse stimulation and a flexible catheter electrode (1.3mm contacts, 15mm spacing, Ad-Tech Medical Instrument Corp). The catheter could be inserted below the lamina to allow access to segments not directly exposed surgically. We confirmed that the data from catheter stimulation was similar to the data recorded with ball electrodes and that exclusion of this data would not substantially change the results (data not shown).

2.4 Data analysis

Data was exported from proprietary intraoperative monitoring software to MATLAB (R2020b) and Python (v3.8) where analysis was performed. . MEPs were quantified using the rectified area under the curve (AUC) calculated in a window between 6.5ms and 75ms after the start of the first stimulation pulse. In order to indicate the absence or presence of MEPs an equivalent estimate of the 50µV threshold was used as is typical in non-invasive studies (Borckardt et al. 2006), resulting in an AUC of 0.33µVs. This value was estimated by regressing AUC onto the peak-peak MEP size.

2.4.1 Statistical analysis

Values are reported as mean ±2×SEM except in cases where the median is used. Non-parametric statistical tests are used throughout (Wilcoxon rank-sum and signed-rank tests, alpha = 0.05).

2.4.2 Artifact rejection

Rejection was based on principal component analysis and confirmation by a human observer and led to 3.6% of MEPs being rejected out of 81,968. The principal components were computed for a specific muscle and electrode location

across multiple stimulation intensities. These principal components captured the shape of the MEPs, and were regressed with each MEP. The root-mean-square of the regression error was then used to rank the responses. This ranking sorted the responses so that the most dissimilar waveform shapes were ranked highest. A manually adjusted sliding scale was then used to reject the highest ranked traces that did not appear physiological under visual inspection.

2.4.3 Midline-lateral comparisons

The MEPs from midline stimulation were compared to lateral stimulation in 3 ways. First, the MEPs for midline and lateral stimulation at 120% of midline threshold were compared within each participant (Fig. 3, insets), using the Wilcoxon rank-sum test, Bonferroni corrected for the number of participants (n = 14). Second, the mean AUC for midline and lateral stimulation for the 14 participants was compared using the Wilcoxon signed-rank test (Fig. 3A). The same method applied to the triceps muscle MEPs (Fig. 3) was applied to the tibialis anterior responses in Fig. 5. Third, to ensure that differences observed in specific muscles at specific segments of stimulation were general trends, all of the responses of the 6 arm and hand muscles were plotted in Fig. 4. The percentage of responses that were larger for lateral stimulation was computed (Fig. 4, inset for each muscle). The third comparison of midline versus lateral stimulation was performed using recruitment curves. The curves were used to estimate thresholds for MEPs and the rate of change of MEPs with stimulation intensity (slope). A function that approximates a linear recruitment cure was used (see section 2.4.6).

2.4.4 Comparison of responses at different cervical segments

All MEPs where the fixed intensity stimulation was used within a single participant were included in this analysis. Due to the exponential nature of MEPs, the AUC was log transformed and plotted to show its relative size. The average AUC across participants was computed by using the geometric mean (Fig. 7A). The similarity in MEPs across segments was measured using the Spearman correlation coefficient, calculated between all segments across muscles for each participant (see Fig. 7B1-2) and then averaged across participants (see Fig. 7B3). To demonstrate similarity across segments, hierarchical agglomerative clustering was applied (Friedman et al. 2001). This procedure recursively calculates the correlation between entries and merges them to create a correlation between clusters which is displayed as a dendrogram. The similarity in MEPs across segments was quantified using the Spearman correlation coefficient,

calculated between all segments across muscles for each participant and then averaged across participants. The merging procedure is based on the linkage metric which was conservatively set to the minimum distance (1 - correlation). We set the cluster cutoff at 70% of the maximum distance.

2.4.5 Estimating the change in MEP produced by moving electrodes midline to lateral versus between segments

Comparisons between movement of electrodes along each axis was possible in 9 participants. The segment of maximum AUC caused by lateral stimulation was first identified for each muscle group; subsequently the difference between MEP sizes at this and neighboring segment(s) was calculated. If two neighboring segments were present, the two differences were calculated and then averaged. Similarly, the difference between the lateral MEP and midline MEP sizes at the same segment was calculated for each muscle. The differences in MEPs were then normalized by distance by dividing MEP values by a generic inter-root length for the rostro-caudal axis and half the transverse cord diameter for the midline versus lateral placement. Distance estimates were derived from a human cadaveric study (Ko et al. 2004), in which inter-root distances (average 12.5mm) and midline to lateral distance (average 6.7mm) were measured. We averaged the normalized MEP sizes across muscles to produce individual lateral-midline and rostro-caudal axis metrics for each participant, to which a Wilcoxon signed-rank test was applied.

2.4.6 Estimation of threshold and slope

Recruitment curves were collected at only one segment per participant because of time constraints. Recruitment curves were fit to enable comparison of slope and threshold across multiple segments. Specifically, the stimulation intensity and AUC relationship was modeled as a softplus function of the form: $\mathrm{y_{j,m,l}} = \mathrm{o_{j,m}} + \frac{\mathrm{b_{j,m,l}}}{\mathrm{k}} \log\left(1 + \mathrm{k}e^{\mathrm{x} - \mathrm{x}^{\mathrm{th}}_{\mathrm{j,m,l}}}\right)$. Where $\mathrm{y_{j,m,l}}$ represents the AUC for a given participant (j), muscle (m) and electrode location (l) for a given stimulation intensity x. Symbols o, b and x^{th} represent the recruitment curve offset, slope and threshold respectively. The parameter k was set to 20 to approximate a linear rectified function while maintaining numerical stability. A fit was performed for every muscle and participant simultaneously for multiple locations on the spinal cord (due to the shared offset). A shared offset was used because in a subset of data sparsely sampled locations did not have unresponsive muscles at any tested intensity. The cost function was defined as the mean absolute error plus the addition of an L1 regularization term and was minimized using MATLAB's implementation of the generalized pattern search algorithm

(Kolda, Lewis, and Torczon 2003). The regularization term was set to 1×10^{-3} and applied only to the slope terms. Regularization forces the slope term to 0 when it does not contribute to the quality of the fit, and this in turn corresponds to cases where the threshold cannot be defined. In order to further filter the estimated parameters the highest stimulation intensity in a given condition had to be at least 0.25mA greater than the estimated threshold. In a small number of conditions (11 of 324) signals saturated and those data points were excluded from the fitting procedure. When only one of the midline or lateral conditions led to a threshold parameter estimate the corresponding midline or lateral estimate was set to the maximum stimulation intensity tested (this is a conservative approach as it likely results in an underestimate of midline thresholds). In order to compare thresholds across the midline and lateral conditions across participants a Wilcoxon signed-rank test was used on the difference between midline and lateral estimates averaged across segments and muscles. The same procedure was used for a comparison of the slope estimates.

3 Results

3.1 Participant recruitment and characteristics

Eighteen participants (nine male and nine female) underwent posterior cervical spine surgery with spinal epidural stimulation (Table 1). Mean age of study participants was 65.2 years (range 48 to 83). 16 patients had chronic symptoms, and two patients had subacute symptoms. 14 patients had clinical signs of myelopathy or myeloradiculopathy (16 had T2 signal change); the remaining patients had radiculopathy alone.

Table 1. Clinical characteristics of participants. See Table 1-1 for associated experiment parameters.

	Age*/Sex	mJOA	Symptom onset	Dominant Syndrome	Unsteady Gait	Pain	Numbness	Weakness	Hyper reflexia		Sphincter dysfunction	T2 signal change
									Upper Extremities	Lower Extremities		
P01	67M	14	Chronic	Myeloradiculopathy	No	Radiating	Yes	Yes	No	No	No	None
P02	48F	14	Chronic	Radiculopathy	No	None	Yes	Yes	Yes	No	No	C2-3, C4-5, C5-6
P03	58M	10	Subacute	Myelopathy	Yes	None	Yes	Yes	No	No	Yes	C4-5, C5-6
P04	54M	17	Chronic	Radiculopathy	No	Radiating	Yes	No	No	No	No	C3-4, C6-7
P05	74F	12	Chronic	Myeloradiculopathy	Yes	Radiating	Yes	Yes	Yes	Yes	No	C3-7

P06	71F	11	Chronic	Myelopathy	No	Radiating	Yes	Yes	Yes	No	No	C4-5, C5-6
P07	62M	10	Chronic	Myelopathy	Yes	None	Yes	Yes	Yes	Yes	No	C6-7
P08	83F	14	Chronic	Myeloradiculopathy	No	Radiating	No	Yes	Yes	Yes	No	C3-4, C4-5, C5-6
P09	72F	12	Subacute	Myelopathy	No	Axial Neck	Yes	Yes	No	No	No	C3-4
P10	70F	10	Chronic	Myelopathy	No	Radiating	Yes	Yes	Yes	No	No	C3-4, C4-5, C6-7
P11	74F	13	Chronic	Myeloradiculopathy	No	Radiating	Yes	Yes	No	No	No	C3-4
P12	50F	11	Chronic	Myeloradiculopathy	No	Radiating	Yes	Yes	Yes	No	No	C5-7
P13	60M	17	Chronic	Radiculopathy	No	None	Yes	No	No	No	No	C3-4
P14	74M	15	Chronic	Myelopathy	Yes	Axial Neck	No	No	Yes	Yes	No	C4-5
P15	75M	16	Chronic	Myeloradiculopathy	Yes	Axial Neck	Yes	Yes	No	No	No	None
P16	54M	17	Chronic	Radiculopathy	No	Radiating	Yes	No	No	No	No	C6-7
P17	71F	11	Chronic	Myeloradiculopathy	Yes	Axial Neck and Radiating	No	Yes	Yes	Yes	No	C3-4
P18	56M	11	Chronic	Myeloradiculopathy	Yes	Axial Neck and Radiating	No	Yes	Yes	Yes	No	C2-3, C3-4, C5-6

*At the time of surgery. mJOA, modified Japanese Orthopaedic Association (mJOA) score.

3.2 Lateral stimulation is more effective than midline stimulation

Comparison of spinal motor evoked potentials (MEPs) to stimulation at midline and lateral locations was performed in 14 participants. We confirmed that placing the electrodes in the lateral position located them over the dorsal root entry zone, where afferent axons enter the spinal cord (Fig. 2). Fig. 3 shows MEPs in response to midline (dark) or lateral (light) stimulation, using an intensity set to 120% of the threshold for midline MEPs. Lateral stimulation of the cervical spinal cord generated larger MEPs than midline stimulation across participants (Fig. 3A; mean midline AUC = 1.14±0.82μVs, lateral AUC = 4.71±2.341.17μVs, Wilcoxon signed-rank test, $p = 0.002$, $n = 14$). These changes correspond to a median increase of 258% in the MEP when stimulating laterally versus at midline. The subplots in Fig. 3B shows raw MEPs of the 14 participants. The upper insets show violin plots of the lateral and midline MEPs for each individual, with asterisks indicating significant differences ($p < 0.05$, Bonferroni corrected Wilcoxon rank sum test). Ten of 14 participants showed significantly increased MEPs with lateral stimulation compared with midline.

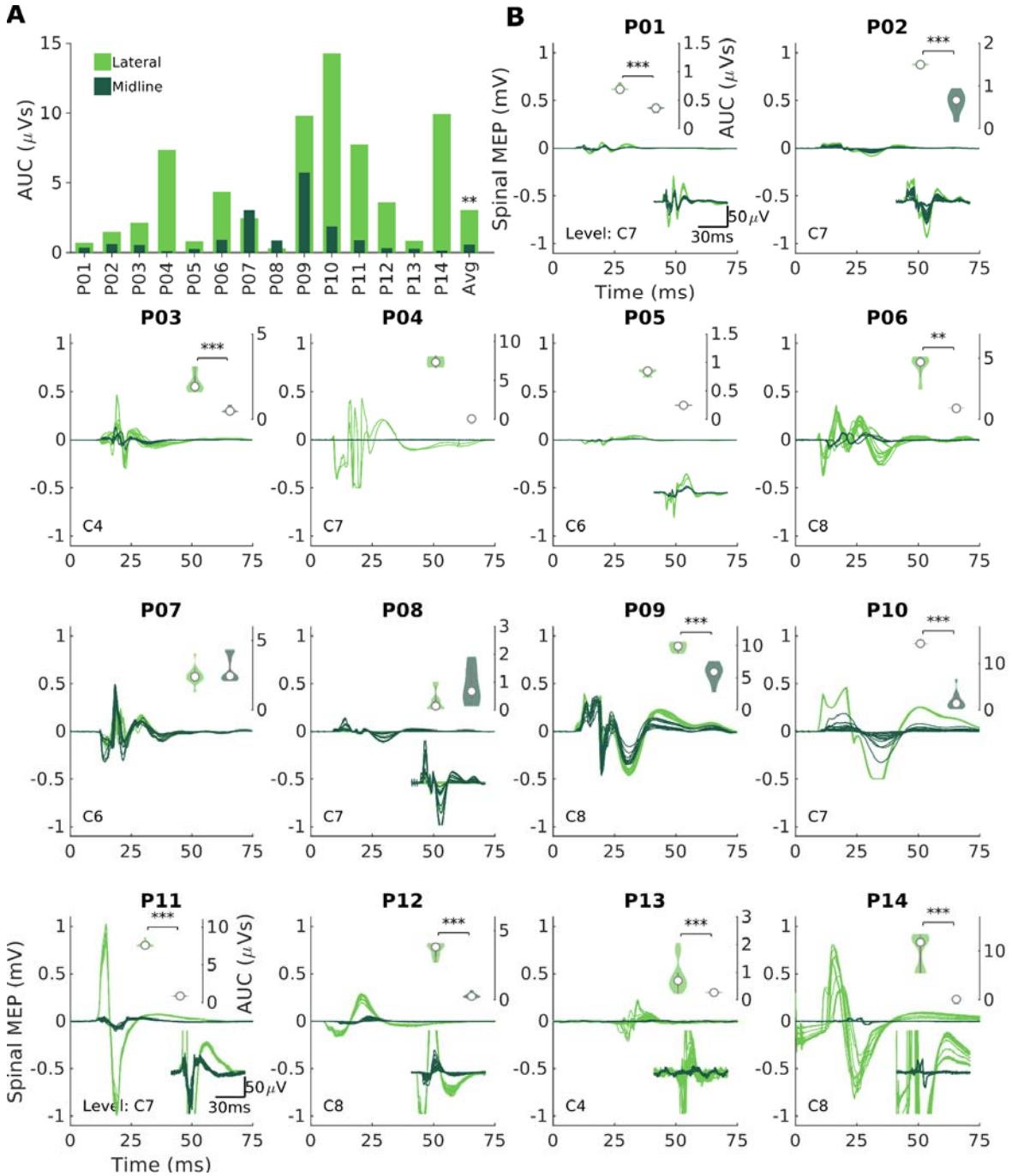

Figure 3. **Lateral stimulation is more effective than midline stimulation**. **(A)** Summary of the rectified area under the curve (AUC) of the triceps muscle at the most caudal segment where a response was present. Midline simulation (dark green) and lateral (light green) stimulation were performed at the fixed intensity for each participant. Motor evoked potentials are shown for the most caudal responsive segment. Lateral stimulation produced consistently larger responses when applied laterally. A signed-rank test was applied between the midline and lateral conditions. Average bar represents the median. **(B)** Individual MEPs that compose the summary plot for individual participants. Bottom inset of each panel represents a magnification of the MEP in cases where the response is small. Top inset of each panel shows a violin plot of AUC (white circle represents the median). Within-participant Wilcoxon rank-sum tests were conducted in individual participants (*$p < 0.05$, **$p < 0.01$, ***$p < 0.001$, Bonferroni corrected for multiple comparisons). Note that for P04, P09 and P10 the signal saturated at 0.5mV due to a limitation of the recording hardware.

The greater effectiveness of lateral compared to midline stimulation was not unique to a specific muscle or any particular segment. Fig. 4 shows each of the six arm muscles in which MEPs were recorded and the six spinal segments that were stimulated. Each dot represents the lateral (y-axis) and midline (x-axis) responses to stimulation at the various segments in each of the participants. All responses above the x = y line represent larger lateral than midline MEPs. On average, across participants, segments and muscles, 91.5% of MEPs were larger when the spinal cord was stimulated laterally.

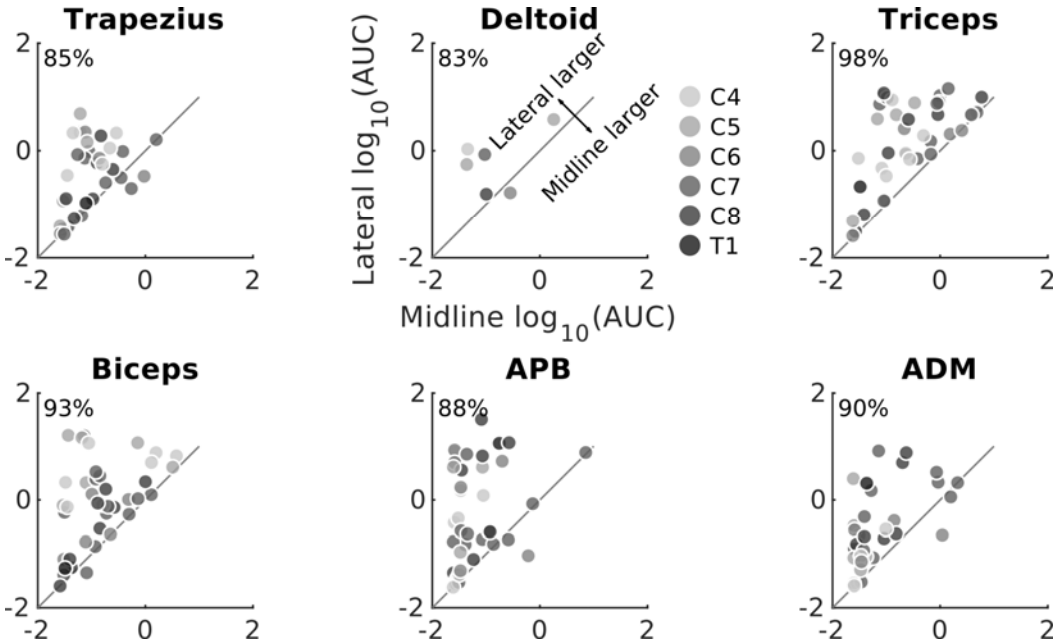

Figure 4. Lateral stimulation is more effective than midline stimulation regardless of stimulation segment or recorded muscle. AUC from all segments and muscles for all participants in whom both midline and lateral stimulation was performed. AUC was larger when stimulation was applied laterally than at midline in the majority of tested cases. The percentage of MEPs that were larger in lateral than midline stimulation is shown in the upper left corner of each plot.

The increased effectiveness of lateral stimulation in the cervical cord was also observed in the leg muscles. Fig. 5A shows the summary of responses for midline (dark) or lateral (light) stimulation. In the 6 out of 14 participants who had tibialis anterior (TA) MEPs in response to cervical stimulation, lateral stimulation generated larger MEPs than midline stimulation (AUC = 0.11±0.10μVs, lateral AUC = 2.43±1.54μVs, Wilcoxon signed-rank test, p = 0.031, n = 6). The subplots in Fig. 5 show raw MEPs of the 6 participants. The upper insets show a violin plot of the lateral and midline MEPs for that individual, with asterisks significant differences ($p < 0.05$, Bonferroni corrected Wilcoxon

rank sum test). All of the 6 participants showed significantly increased MEPs with lateral stimulation compared with midline.

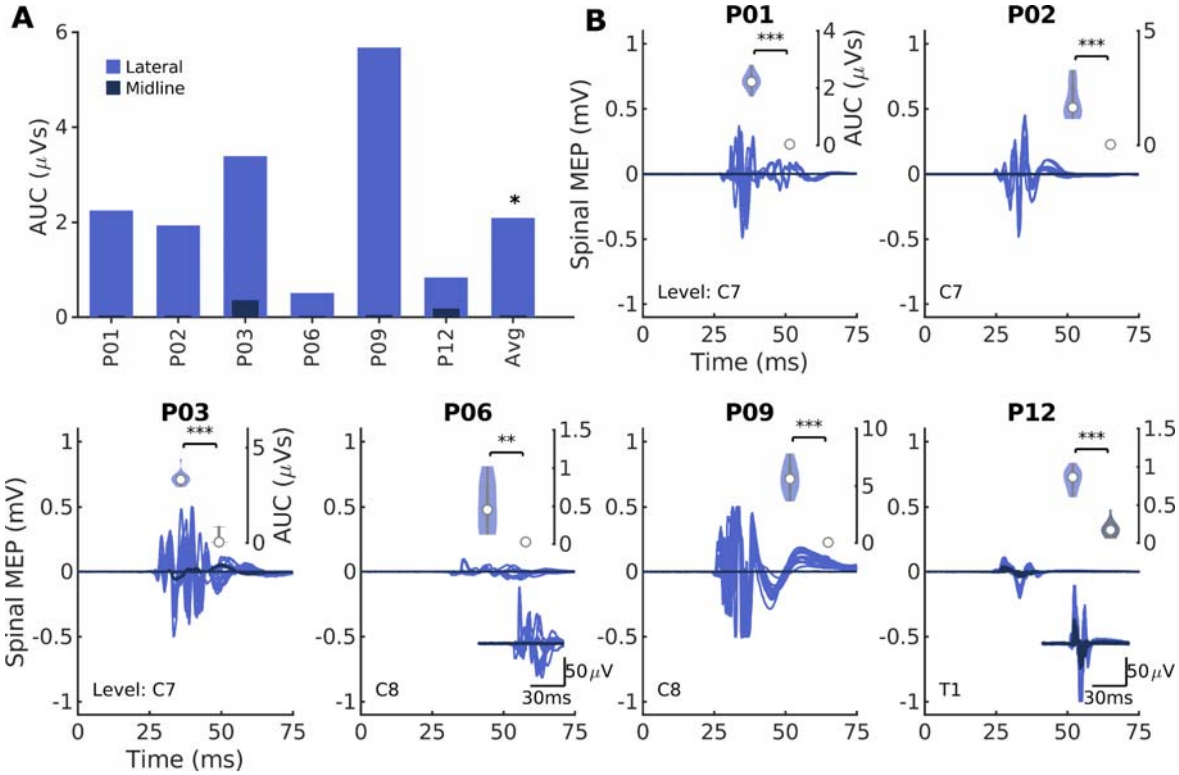

Figure 5. A subset of participants display activation in their leg muscles when stimulation is applied in the cervical cord. (A) Summary of the rectified area under the curve (AUC) of the tibialis anterior (TA) muscle at the most caudal segment where a response was present. Midline simulation (dark blue) and lateral (light blue) stimulation was performed at the fixed intensity for each participant. Motor evoked potentials (MEPs) are shown for the most caudal responsive segment. In a subset of participants that display activation of tibialis anterior (AUC greater than 0.33μVs), lateral stimulation produced consistently larger responses. A signed-rank test was applied between the midline and lateral conditions; the average bar represents the median value. **(B)** Individual spinal MEPs that compose the summary plot for individual participants. Bottom inset of each panel represents a magnification of the MEP in cases where the response was small. Top inset of each panel shows a violin plot of AUC (white circle represents the median). Within participant Wilcoxon rank-sum tests were conducted in individual participants (*$p < 0.05$, **$p < 0.01$, ***$p < 0.001$, Bonferroni corrected for multiple comparisons). Note that for P09 the signal saturated at 0.5mV due to a limitation of the recording hardware.

3.3 Lateral MEPs are larger due to lower thresholds and steeper recruitment curves

The increased effectiveness of lateral stimulation may be driven by a reduction in the threshold for recruitment, an increase in the rate of change of MEP size with stimulation intensity (slope of the recruitment), or both. Recruitment curves were fitted in order to estimate these parameters directly from data where multiple stimulation intensities were tested at the same segment (e.g. Fig. 1C, C7). Examples of the recruitment curve threshold and slope estimation

procedure for the triceps muscle of two participants are shown in Fig. 6A for midline and lateral stimulation. Across participants, averaged threshold increased 126% for midline stimulation over lateral stimulation, indicating higher stimulus intensity was needed to evoke an MEP ($p = 2\times10^{-4}$, Wilcoxon signed-rank test, n = 13; Fig. 6B). The rate of increase of MEP size with stimulation intensity was also influenced by the site of stimulation, with a median increase in the slope of 65% for lateral stimulation compared to midline stimulation ($p = 0.027$, Wilcoxon signed-rank test, n = 13; Fig. 6C). Thus, lateral stimulation was more effective than midline stimulation both because of a lower threshold and because of an increased slope of the recruitment curve.

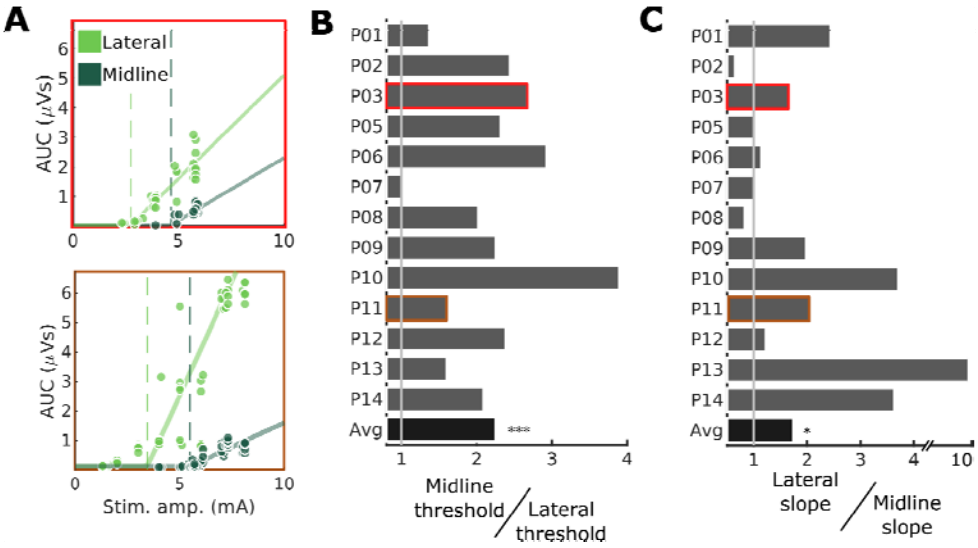

Figure 6. Larger lateral MEPs driven by both a reduction in threshold and increase in slope. **(A)** The threshold of muscle activation was determined by fitting functions to sections of data where multiple stimulation intensities were used. Circles indicate individual data points (light green, lateral; dark green, midline), solid lines show example fitted functions, and dashed lines show estimates of threshold. **(B)** The relative efficacy of lateral stimulation can be summarized as midline threshold ÷ lateral threshold (lower lateral threshold indicates higher lateral efficacy). The majority of participants showed lower lateral than midline threshold. **(C)** Lateral to midline slope ratio (lateral slope ÷ midline slope). The majority of participants showed steeper recruitment slopes from stimulation at lateral sites. Note that one participant has been omitted (P04) as there was insufficient range in tested stimulation intensities to perform model fitting. Average bar represents the median.

3.4 Cervical dorsal stimulation evokes MEPs in muscles innervated at that segment with spread

While we predicted a sharp difference in responses between midline and lateral stimulation, we expected smaller differences with movement between cervical segments along the rostro-caudal axis (Fig. 1B). MEPs were recorded in arm and leg muscles after a fixed intensity stimulation at 6 different spinal segments (C4-T1). Fig. 7A shows MEP values for each muscle with stimulation at segments C4 to T1. Individual participants are represented by the faint lines, and the group average for each muscle by the bold lines. The dashed lines indicate a threshold for the presence of MEPs. The largest MEPs were observed in the muscles innervated at the stimulated segment. For example, biceps activation was dominant at C4 and C5, triceps at C6 and C7, and APB at C8 and T1. Triceps MEPs were present at all segments except for T1. Additionally, as shown in Fig. 3, some participants had MEPs in the legs, although those were always smaller.

The patterns of responses are likely to reveal how related each segment is to the other segments. To determine this, we calculated the correlation between segments of MEPs from all muscles. Figures 7B1 or B2 show the results of all the individual participants that had stimulation at the two segments indicated on the axes. Each dot corresponds to the MEP for an individual muscle, and all the arm and hand muscles for an individual are used to create a linear correlation represented by a line. By averaging these correlations across participants (Fig. 7B3), we were able to examine the similarity of muscle responses across segments without the confound of across-participant variability. MEPs largely fell into two distinct clusters, C4-C6 and C7-T1. We used a clustering algorithm to show these relationships; the correlation within the C4-C6 cluster averaged 0.7, while the C7-T1 averaged 0.9. The correlation between the two clusters was 0.5. Thus, each of these two clusters is strongly related internally, with much lower correlations between them.

Our goal was to understand the organization of the cervical spinal cord in health, but the study was performed in people with myelopathy. To control for the effect of injury to the spinal cord, we performed lateral stimulation on the less affected side. In addition, we performed an analysis similar to Fig. 7 but excluding responses in all segments where T2 signal change was present. This did not change the pattern of responses significantly (average correlation between MEP size with and without T2 signal change segments excluded r = 0.91, Extended Fig. 7-1). This high

correlation suggests that the patterns of muscle activation from cervical spinal cord stimulation were driven largely by the activation of intrinsic circuits that were spared by the effects of myelopathy.

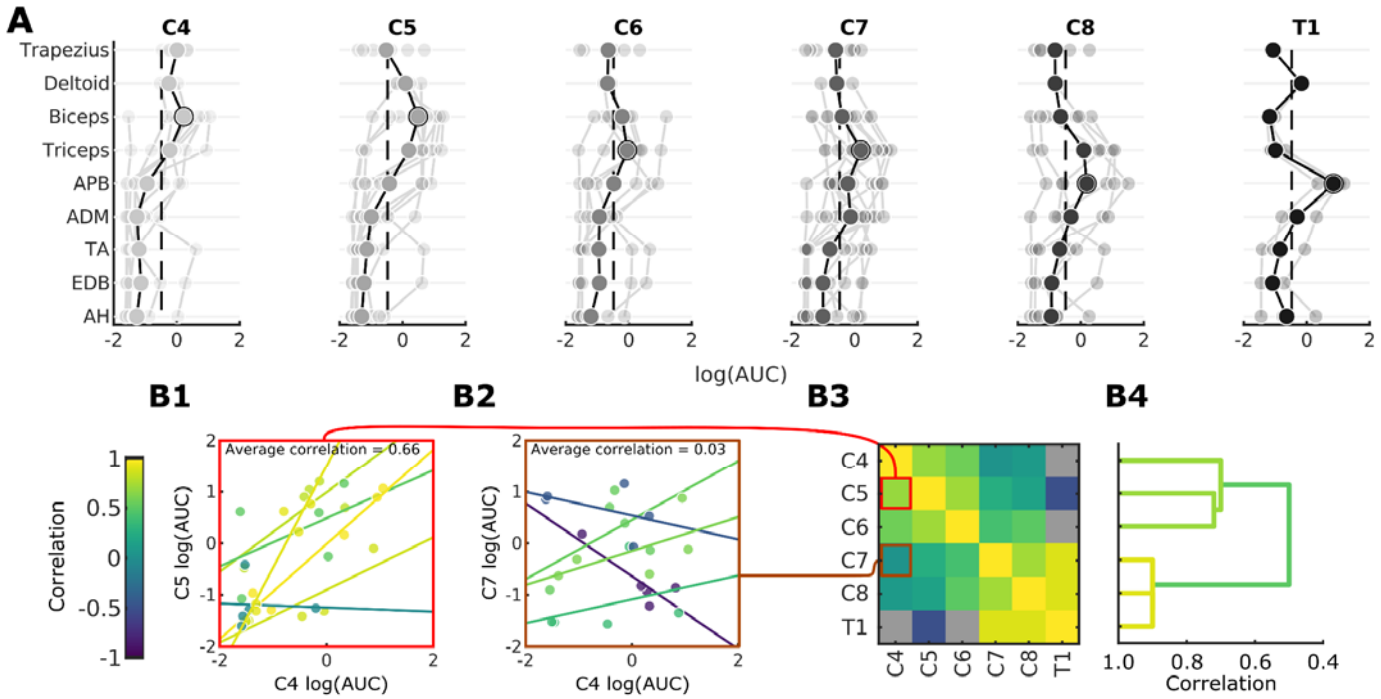

Figure 7. Rostral-caudal distribution of MEPs show expected peak responses with spread to adjacent segments and unexpected strong correlations within the upper (C4-C6) versus lover (C7-T1) cervical spinal cord. (A) MEPs for each of the recorded muscles with stimulation are shown for lateral stimulation at segments C4-T1. The data are plotted on a log scale with the average in bold. Faint lines represent individual participant data (n = 18). Dashed line (0.33µVs) indicates a threshold for presence of MEPs (see Methods). Equivalent figure with T2 signal change segments excluded is shown in Figure 7-1. **(B)** Within-participant similarity (correlation) of muscle responses at different segments, averaged across participants. **(B1-2)** Example AUC data correlations when comparing C4 to C5 **(B1)** or to a more distant C7 **(B2)**. Nearby segments are highly correlated for the majority of participants (colors represent different participants), while more distant segments are not. **(B3)** Muscle activation appears to separate into two distinct clusters: higher cervical (C4-C6) areas produce muscle activation highlight correlated to other higher cervical segments, but distinct from lower cervical segments (C7-C8, T1). **(B4)** Dendrogram constructed from hierarchical clustering of (B3). Individual pairs of correlations are merged into clusters, and the maximum correlation between the entries in these clusters is represented by the width of the merge. Colors represent the maximum correlation within distinct clusters (see methods).

3.5 An actionable map for epidural stimulation of the cervical spinal cord.

Fig. 8A summarizes the muscles activated by stimulation at each cervical segment. Circle area corresponds to the percent of total MEP size contributed by specific muscles (designated by color), and the darkness of the circle corresponds to the number of participants. Only MEPs that were on average greater than 0.33µVs are shown,

highlighting the dominant muscles at each segment. While all lateral stimulation sites met this threshold, the only midline response above this threshold was the triceps MEP at C7. This map demonstrates the activation of specific muscles at each segment of the cervical spinal cord.

Differences between MEP size were larger between midline and lateral stimulation within segments than between segments. To quantify this, we determined change in MEPs as a function of distance – how much does the MEP change with each millimeter that the stimulating electrode was moved in each direction. The average MEP size was reduced at a rate of 0.39±0.24μVs/mm when moving from lateral to midline. On the other hand, MEP size from stimulation of neighboring segments was reduced at a lower rate of 0.15±0.08μVs/mm. The rate of change was more than double for medial-lateral electrode position compared with rostro-caudal position, and this difference was highly significant (p = 0.008, n = 9).

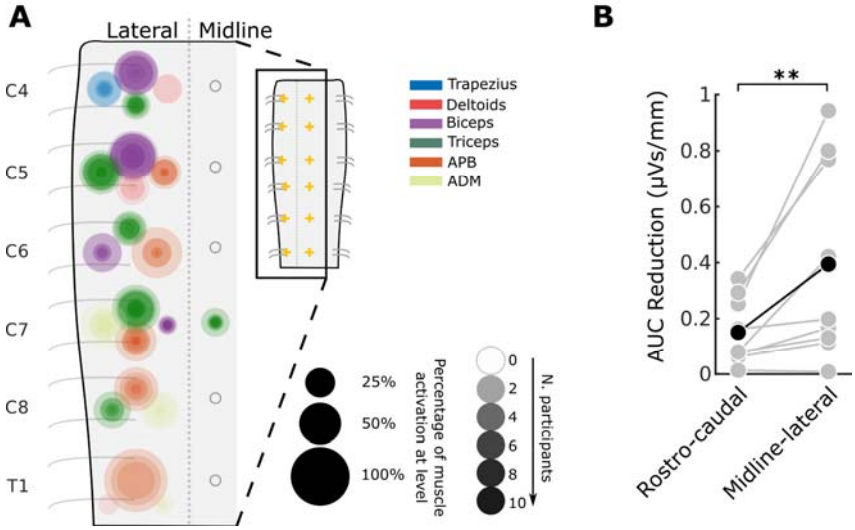

Figure 8. An actionable map for epidural stimulation of the cervical spinal cord. (A) Area of overlaid circles represents the rectified area under the curve (AUC) of individual participants. Activation is only drawn when the across-participant average AUC is greater than 0.33μVs (see methods). Empty circles represent no muscle activation reached this threshold. (Data shown here is a summarized representation of data shown in Fig. 7A). Inset: Crosses mark locations of stimulation. **(B)** AUC reduction is greatest when traversing in the midline-lateral, as compared to in the rostro-caudal axis when averaging across participants (black), as well as for the majority of participants (gray). See Fig. 1B and methods for normalization procedure.

4 Discussion

The results of our stimulation mapping provide evidence for the underlying organization of the human cervical spinal cord. The largest changes in stimulus response were observed between midline and lateral locations, which is likely due to the recruitment of large-diameter afferents laterally at the dorsal root entry zone. Sequential stimulation at multiple levels along the rostro-caudal axis was used to evaluate segmental organization of the cord and resulted in more subtle differences in motor responses than did transition from lateral to midline stimulation, suggesting the presence of strong overlap with adjoining segments. Clustering of these responses was particularly strong with the upper cervical cord (C4, C5, C6) and lower cervical segments (C7, C8, T1). Finally, we observed MEPs arising from distant segments of the cervical spinal cord and from leg muscles, indicating potential activation of propriospinal connections (Dietz 2002; Islam et al. 2020). Thus, the summary map of responses (Fig. 8A) provides a guide to target specific muscles via dorsal cervical spinal cord stimulation but also a functional map of how stimulation is expected to affect non-targeted muscles as well.

While the observed differences between midline and lateral stimulation and between neighboring segments have support in the literature, the finding of clustering within the upper and lower cervical enlargement is novel. Unexpected spread of responses beyond the stimulated segment (Schirmer et al. 2011) even with intraspinal cervical stimulation (Sunshine et al. 2013) and activation of leg muscles from stimulation of the cervical cord have been reported (Dimitrijevic et al. 1980; Schirmer et al. 2011; Sabbahi et al. 2014; Kato, Nishihara, and Nishimura 2020). Consistent with these findings we observed long-range activation within the spinal cord, for example triceps activation with C4 stimulation and leg activation with cervical stimulation. Such activation cannot be explained by known locations of motor pools and intermingling of motoneuron cell bodies (Chiken, Hatanaka, and Tokuno 2001; Jenny and Inukai 1983) and suggests the presence of long distance connections within the cervical enlargement (Lamotte 1977; Pierrot-Deseilligny 2002; Atik et al. 2019) and between the cervical and lumbar enlargements (Dietz 2002; Zehr and Duysens 2004; Ferris, Huang, and Kao 2006; Balter and Zehr 2007; Masugi et al. 2019). Clustering of upper compared with lower cervical responses may highlight a difference in stimulation technique or study population. In the monkey cervical cord, Greiner et al. demonstrated separation of biceps and triceps by stimulating between the C6 and C8 segments. However, consistent with human data also described by Greiner et al., our results suggest no such

separation in bipedal humans compared with quadrupedal macaques. Rather, our results suggest a division between the muscles of the hand and muscles of the arm. This organization could be engaged to foster adaptive patterns of arm and hand muscle activation.

We expect that the breadth of muscle activation with stimulation across segments (for example, strong activation of biceps from stimulation at C4) is mediated by the spread of afferent connections into the spinal cord overlapping with the spread of efferent pathways out of the spinal cord. Some observed responses may be partially driven by non-biological spread of the electric field across levels (Rattay, Minassian, and Dimitrijevic 2000), but the presence of leg muscle MEPs provides strong evidence that spinal cord pathways represent a critical mechanism. Additionally, we observe a much larger change in MEP size when electrodes are moved in the midline-lateral orientation than when they are moved in the rostral-caudal orientation, suggestive of the limitations of current spread.

While the operating room provides a unique experimental setting, it may also limit the generalizability of our findings. Participants had myelopathy and/or radiculopathy, and these pathologies may affect axonal conduction, neuronal signaling, or synaptic connectivity. We did, however, perform a sensitivity analysis for the effect of cervical injury by excluding the segments with T2 hyperintensity, indicative of myelomalacia; excluding these levels did not change the overall structure of the activation map. MEP size may also have been affected by general anesthesia; however, all participants were maintained on total intravenous anesthesia, consistent with standard operative and intraoperative neuromonitoring conditions; in all of our experiments we observed clear, reproducible responses at multiple tested segments. Importantly, anesthetic conditions had reached a steady state during recording, and no changes were made during the experiment. Participants were tested in an immobilized prone position, so we were not able to address how epidural stimulation can be used to generate movement (Greiner et al. 2021; Kato, Nishihara, and Nishimura 2020; Barra et al. 2021) or how MEPs interact with body position (Marsden, Merton, and Morton 1981; Knikou 2006; Knikou et al. 2009; Danner et al. 2016). In future studies these limitations may be addressed in alternative experimental settings either non-invasively or with implanted leads.

The map of muscle responses to cervical epidural stimulation can facilitate better understanding of spinal circuits and help target interventions. Stimulation of the cervical spinal cord may reveal patterns of activation, whether mediated by motor primitives or complex movements. In addition to single or short trains of stimuli, longer trains and/or

multisite stimulation may help to reveal these motor programs. Multiple sites of stimulation may be needed to activate the desired circuit activation or movement. This stimulation may be used to activate movement directly or to strengthen weak spinal circuits. Thus, the map serves to identify the cervical circuits that control dexterity and to target neural repair to damaged connections.

Conflict of interest

Jason B. Carmel is a Founder and stock holder in BackStop Neural and a scientific advisor for SharperSense. Michael S. Virk has been a consultant and has received honorarium from Depuy Synthes, Globus Medical and BrainLab. Noam Y. Harel is a consultant for RubiconMD. K. Daniel Riew: Board of Directors: Global Spine Journal (Nonfinancial), NASS (Nonfinancial); Consulting: Happe Spine (Nonfinancial), Nuvasive; Royalties: Biomet; Speaking and/or Teaching Arrangements: Biomet, Medtronic (Travel Expense Reimbursement); Stock Ownership: Amedica, Axiomed, Benvenue, Expanding Orthopedics, Osprey, Paradigm Spine, Spinal Kinetics, Spineology, Vertiflex. The rest of the coauthors have nothing to disclose.

Acknowledgements:

Sources of financial support: This study was funded by the National Institutes of Health (1R01NS124224); and the Travis Roy Foundation Boston, MA (Investigator Initiated).

We thank neurologists P. Kent, H. Choi, M. Bell (The Och Spine Hospital At New York Presbyterian Hospital) and intraoperative monitoring technologists N. Patel, Z. Moheet (Weill Cornell Medicine), Joe Elliott, Brian Demboski, Kelley Wichman, Susannah Storms, Meghan Mullaney, Evance Desriviere (The Och Spine Hospital At New York Presbyterian Hospital) for monitoring patient safety during the experiments, as well as help with running the experiments. We also thank S. Oh (Columbia University), E. Wong (Brainlab AG) and Brainlab AG for help with image processing and M. Vulapalli, C. Mykolajtchuk, M. Michael (Weill Cornell Medicine) for help in administrative matters.

8 References

Anderson, Kim D. 2004. “Targeting Recovery: Priorities of the Spinal Cord-Injured Population.” *Journal of Neurotrauma* 21 (10): 1371–83. https://doi.org/10.1089/neu.2004.21.1371.

Angeli, Claudia A., Maxwell Boakye, Rebekah A. Morton, Justin Vogt, Kristin Benton, Yangshen Chen, Christie K. Ferreira, and Susan J. Harkema. 2018. "Recovery of Over-Ground Walking after Chronic Motor Complete Spinal Cord Injury." *New England Journal of Medicine* 379 (13): 1244–50. https://doi.org/10.1056/NEJMoa1803588.

Atik, Ahmet Fatih, Evan Calabrese, Robert Gramer, Syed M. Adil, Shervin Rahimpour, Promila Pagadala, G. Allan Johnson, and Shivanand P. Lad. 2019. "Structural Mapping with Fiber Tractography of the Human Cuneate Fasciculus at Microscopic Resolution in Cervical Region." *NeuroImage* 196 (August): 200–206. https://doi.org/10.1016/j.neuroimage.2019.04.030.

Balter, Jaclyn E., and E. Paul Zehr. 2007. "Neural Coupling Between the Arms and Legs During Rhythmic Locomotor-Like Cycling Movement." *Journal of Neurophysiology* 97 (2): 1809–18. https://doi.org/10.1152/jn.01038.2006.

Barra, B., S. Conti, M. G. Perich, K. Zhuang, G. Schiavone, F. Fallegger, K. Galan, et al. 2021. "Epidural Electrical Stimulation of the Cervical Dorsal Roots Restores Voluntary Upper Limb Control in Paralyzed Monkeys." https://doi.org/10.1101/2020.11.13.379750.

Bollini, Carlos A., and Jaime A. Wikinski. 2006. "Anatomical Review of the Brachial Plexus." *Techniques in Regional Anesthesia and Pain Management*, Peripheral Nerve Blocks: A View from Argentina, I, 10 (3): 69–78. https://doi.org/10.1053/j.trap.2006.07.006.

Borckardt, Jeffrey J., Ziad Nahas, Jejo Koola, and Mark S. George. 2006. "Estimating Resting Motor Thresholds in Transcranial Magnetic Stimulation Research and Practice: A Computer Simulation Evaluation of Best Methods." *The Journal of ECT* 22 (3): 169–75. https://doi.org/10.1097/01.yct.0000235923.52741.72.

Brendler, Samuel J. 1968. "The Human Cervical Myotomes: Functional Anatomy Studied at Operation." *Journal of Neurosurgery* 28 (2): 105–11. https://doi.org/10.3171/jns.1968.28.2.0105.

Capogrosso, Marco, Nikolaus Wenger, Stanisa Raspopovic, Pavel Musienko, Janine Beauparlant, Lorenzo Bassi Luciani, Grégoire Courtine, and Silvestro Micera. 2013. "A Computational Model for Epidural Electrical Stimulation of Spinal Sensorimotor Circuits." *Journal of Neuroscience* 33 (49): 19326–40. https://doi.org/10.1523/JNEUROSCI.1688-13.2013.

Carhart, M.R., Jiping He, R. Herman, S. D'Luzansky, and W.T. Willis. 2004. "Epidural Spinal-Cord Stimulation Facilitates Recovery of Functional Walking Following Incomplete Spinal-Cord Injury." *IEEE Transactions on Neural Systems and Rehabilitation Engineering* 12 (1): 32–42. https://doi.org/10.1109/TNSRE.2003.822763.

Chiken, S., N. Hatanaka, and H. Tokuno. 2001. "Distribution of Median, Ulnar and Radial Motoneurons in the Monkey Spinal Cord: A Retrograde Triple-Labeling Study." *Neuroscience Letters* 307 (3): 143–46. https://doi.org/10.1016/s0304-3940(01)01918-8.

Danner, Simon M., Ursula S. Hofstoetter, Brigitta Freundl, Heinrich Binder, Winfried Mayr, Frank Rattay, and Karen Minassian. 2015. "Human Spinal Locomotor Control Is Based on Flexibly Organized Burst Generators." *Brain: A Journal of Neurology* 138 (Pt 3): 577–88. https://doi.org/10.1093/brain/awu372.

Danner, Simon M., Matthias Krenn, Ursula S. Hofstoetter, Andrea Toth, Winfried Mayr, and Karen Minassian. 2016. "Body Position Influences Which Neural Structures Are Recruited by Lumbar Transcutaneous Spinal Cord Stimulation." *PloS One* 11 (1): e0147479. https://doi.org/10.1371/journal.pone.0147479.

Dietz, Volker. 2002. "Do Human Bipeds Use Quadrupedal Coordination?" *Trends in Neurosciences* 25 (9): 462–67. https://doi.org/10.1016/S0166-2236(02)02229-4.

Dimitrijevic, M. R., J. Faganel, P. C. Sharkey, and A. M. Sherwood. 1980. "Study of Sensation and Muscle Twitch Responses to Spinal Cord Stimulation." *International Rehabilitation Medicine* 2 (2): 76–81. https://doi.org/10.3109/09638288009163961.

Dimitrijevic, M. R., Y. Gerasimenko, and M. M. Pinter. 1998. "Evidence for a Spinal Central Pattern Generator in Humans." *Annals of the New York Academy of Sciences* 860 (November): 360–76. https://doi.org/10.1111/j.1749-6632.1998.tb09062.x.

Ferris, Daniel P., Helen J. Huang, and Pei-Chun Kao. 2006. "Moving the Arms to Activate the Legs." *Exercise and Sport Sciences Reviews* 34 (3): 113–20. https://doi.org/10.1249/00003677-200607000-00005.

Freyvert, Yevgeniy, Nicholas Au Yong, Erika Morikawa, Sharon Zdunowski, Melanie E. Sarino, Yury Gerasimenko, V. Reggie Edgerton, and Daniel C. Lu. 2018. "Engaging Cervical Spinal Circuitry with Non-Invasive Spinal Stimulation and Buspirone to Restore Hand Function in Chronic Motor Complete Patients." *Scientific Reports* 8 (1): 15546. https://doi.org/10.1038/s41598-018-33123-5.

Friedman, Jerome, Trevor Hastie, Robert Tibshirani, and others. 2001. *The Elements of Statistical Learning*. Vol. 1.

10. Springer series in statistics New York.
Gill, Megan L., Peter J. Grahn, Jonathan S. Calvert, Margaux B. Linde, Igor A. Lavrov, Jeffrey A. Strommen, Lisa A. Beck, et al. 2018. "Neuromodulation of Lumbosacral Spinal Networks Enables Independent Stepping after Complete Paraplegia." *Nature Medicine* 24 (11): 1677–82. https://doi.org/10.1038/s41591-018-0175-7.
Greiner, Nathan, Beatrice Barra, Giuseppe Schiavone, Henri Lorach, Nicholas James, Sara Conti, Melanie Kaeser, et al. 2021. "Recruitment of Upper-Limb Motoneurons with Epidural Electrical Stimulation of the Cervical Spinal Cord." *Nature Communications* 12 (1): 435. https://doi.org/10.1038/s41467-020-20703-1.
Hofstoetter, Ursula S., Brigitta Freundl, Heinrich Binder, and Karen Minassian. 2018. "Common Neural Structures Activated by Epidural and Transcutaneous Lumbar Spinal Cord Stimulation: Elicitation of Posterior Root-Muscle Reflexes." *PloS One* 13 (1): e0192013. https://doi.org/10.1371/journal.pone.0192013.
Inanici, Fatma, Lorie N. Brighton, Soshi Samejima, Christoph P. Hofstetter, and Chet T. Moritz. 2021. "Transcutaneous Spinal Cord Stimulation Restores Hand and Arm Function After Spinal Cord Injury." *IEEE Transactions on Neural Systems and Rehabilitation Engineering* 29: 310–19. https://doi.org/10.1109/TNSRE.2021.3049133.
Islam, Md. Anamul, Morad Zaaya, Erin Comiskey, Joseph Demetrio, Amanda O'Keefe, Nicole Palazzo, Timothy S. Pulverenti, and Maria Knikou. 2020. "Modulation of Soleus H-Reflex Excitability Following Cervical Transspinal Conditioning Stimulation in Humans." *Neuroscience Letters* 732 (July): 135052. https://doi.org/10.1016/j.neulet.2020.135052.
Jenny, A. B., and J. Inukai. 1983. "Principles of Motor Organization of the Monkey Cervical Spinal Cord." *Journal of Neuroscience* 3 (3): 567–75. https://doi.org/10.1523/JNEUROSCI.03-03-00567.1983.
Kato, Kenji, Yoko Nishihara, and Yukio Nishimura. 2020. "Stimulus Outputs Induced by Subdural Electrodes on the Cervical Spinal Cord in Monkeys." *Journal of Neural Engineering* 17 (1): 016044. https://doi.org/10.1088/1741-2552/ab63a3.
Knikou, Maria. 2006. "Effects of Changes in Hip Position on Actions of Spinal Inhibitory Interneurons in Humans." *The International Journal of Neuroscience* 116 (8): 945–61. https://doi.org/10.1080/00207450600675167.
Knikou, Maria, Claudia A. Angeli, Christie K. Ferreira, and Susan J. Harkema. 2009. "Soleus H-Reflex Gain, Threshold, and Amplitude as Function of Body Posture and Load in Spinal Cord Intact and Injured Subjects." *International Journal of Neuroscience* 119 (11): 2056–73. https://doi.org/10.1080/00207450903139747.
Ko, H.-Y., J. H. Park, Y. B. Shin, and S. Y. Baek. 2004. "Gross Quantitative Measurements of Spinal Cord Segments in Human." *Spinal Cord* 42 (1): 35–40. https://doi.org/10.1038/sj.sc.3101538.
Kolda, Tamara G., Robert Michael Lewis, and Virginia Torczon. 2003. "Optimization by Direct Search: New Perspectives on Some Classical and Modern Methods." *SIAM Review* 45 (3): 385–482.
Kumru, Hatice, África Flores, María Rodríguez-Cañón, Victor R. Edgerton, Loreto García, Jesús Benito-Penalva, Xavier Navarro, Yury Gerasimenko, Guillermo García-Alías, and Joan Vidal. 2021. "Cervical Electrical Neuromodulation Effectively Enhances Hand Motor Output in Healthy Subjects by Engaging a Use-Dependent Intervention." *Journal of Clinical Medicine* 10 (2): 195. https://doi.org/10.3390/jcm10020195.
Lamotte, Carole. 1977. "Distribution of the Tract of Lissauer and the Dorsal Root Fibers in the Primate Spinal Cord." *Journal of Comparative Neurology* 172 (3): 529–61. https://doi.org/10.1002/cne.901720308.
Lloyd, D. P. C. 1943. "Reflex Action in Relation to Pattern and Peripheral Source of Afferent Stimulation." *Journal of Neurophysiology* 6: 111–19.
Lu, Daniel C., V. Reggie Edgerton, Morteza Modaber, Nicholas AuYong, Erika Morikawa, Sharon Zdunowski, Melanie E. Sarino, et al. 2016. "Engaging Cervical Spinal Cord Networks to Reenable Volitional Control of Hand Function in Tetraplegic Patients." *Neurorehabilitation and Neural Repair* 30 (10): 951–62. https://doi.org/10.1177/1545968316644344.
Marsden, C. D., P. A. Merton, and H. B. Morton. 1981. "Human Postural Responses." *Brain: A Journal of Neurology* 104 (3): 513–34. https://doi.org/10.1093/brain/104.3.513.
Masugi, Yohei, Atsushi Sasaki, Naotsugu Kaneko, and Kimitaka Nakazawa. 2019. "Remote Muscle Contraction Enhances Spinal Reflexes in Multiple Lower-Limb Muscles Elicited by Transcutaneous Spinal Cord Stimulation." *Experimental Brain Research* 237 (7): 1793–1803. https://doi.org/10.1007/s00221-019-05536-9.
Mishra, Asht M., Ajay Pal, Disha Gupta, and Jason B. Carmel. 2017. "Paired Motor Cortex and Cervical Epidural Electrical Stimulation Timed to Converge in the Spinal Cord Promotes Lasting Increases in Motor Responses." *The Journal of Physiology* 595 (22): 6953–68. https://doi.org/10.1113/JP274663.
Moritz, Chet T., Timothy H. Lucas, Steve I. Perlmutter, and Eberhard E. Fetz. 2007. "Forelimb Movements and

Muscle Responses Evoked by Microstimulation of Cervical Spinal Cord in Sedated Monkeys." *Journal of Neurophysiology* 97 (1): 110–20. https://doi.org/10.1152/jn.00414.2006.

Pal, Ajay, HongGeun Park, Aditya Ramamurthy, Ahmet S. Asan, Thelma Bethea, Meenu Johnkutty, and Jason B. Carmel. 2021. "Spinal Cord Associative Plasticity Improves Forelimb Sensorimotor Function after Cervical Injury." https://doi.org/10.1101/2020.12.07.398289.

Pierrot-Deseilligny, Emmanuel. 2002. "Propriospinal Transmission of Part of the Corticospinal Excitation in Humans." *Muscle & Nerve* 26 (2): 155–72. https://doi.org/10.1002/mus.1240.

Rattay, F., K. Minassian, and M. R. Dimitrijevic. 2000. "Epidural Electrical Stimulation of Posterior Structures of the Human Lumbosacral Cord: 2. Quantitative Analysis by Computer Modeling." *Spinal Cord* 38 (8): 473–89. https://doi.org/10.1038/sj.sc.3101039.

Renshaw, Birdsey. 1940. "Activity in the Simplest Spinal Reflex Pathways." *Journal of Neurophysiology* 3 (5): 373–87. https://doi.org/10.1152/jn.1940.3.5.373.

Sabbahi, Mohamed A., Selda Uzun, Fikriye Ovak Bittar, and Yesim Sengul. 2014. "Similarities and Differences in Cervical and Thoracolumbar Multisegmental Motor Responses and the Combined Use for Testing Spinal Circuitries." *The Journal of Spinal Cord Medicine* 37 (4): 401–13. https://doi.org/10.1179/2045772313Y.0000000157.

Schirmer, Clemens M., Jay L. Shils, Jeffrey E. Arle, G. Rees Cosgrove, Peter K. Dempsey, Edward Tarlov, Stephan Kim, et al. 2011. "Heuristic Map of Myotomal Innervation in Humans Using Direct Intraoperative Nerve Root Stimulation." *Journal of Neurosurgery. Spine* 15 (1): 64–70. https://doi.org/10.3171/2011.2.SPINE1068.

Sharpe, Abigail N, and Andrew Jackson. 2014. "Upper-Limb Muscle Responses to Epidural, Subdural and Intraspinal Stimulation of the Cervical Spinal Cord." *Journal of Neural Engineering* 11 (1): 016005. https://doi.org/10.1088/1741-2560/11/1/016005.

Snoek, G. J., M. J. IJzerman, H. J. Hermens, D. Maxwell, and F. Biering-Sorensen. 2004. "Survey of the Needs of Patients with Spinal Cord Injury: Impact and Priority for Improvement in Hand Function in Tetraplegics." *Spinal Cord* 42 (9): 526–32. https://doi.org/10.1038/sj.sc.3101638.

Sunshine, Michael D., Frances S. Cho, Danielle R. Lockwood, Amber S. Fechko, Michael R. Kasten, and Chet T. Moritz. 2013. "Cervical Intraspinal Microstimulation Evokes Robust Forelimb Movements before and after Injury." *Journal of Neural Engineering* 10 (3): 036001. https://doi.org/10.1088/1741-2560/10/3/036001.

Tubbs, R. Shane, Diala El-Zammar, Marios Loukas, Ayhan Cömert, and Aaron A. Cohen-Gadol. 2009. "Intradural Cervical Root Adjacent Interconnections in the Normal, Prefixed, and Postfixed Brachial Plexus: Laboratory Investigation." *Journal of Neurosurgery: Spine* 11 (4): 413–16. https://doi.org/10.3171/2009.4.SPINE09104.

Wagner, Fabien B., Jean-Baptiste Mignardot, Camille G. Le Goff-Mignardot, Robin Demesmaeker, Salif Komi, Marco Capogrosso, Andreas Rowald, et al. 2018. "Targeted Neurotechnology Restores Walking in Humans with Spinal Cord Injury." *Nature* 563 (7729): 65–71. https://doi.org/10.1038/s41586-018-0649-2.

Wu, Yu Kuang, Jonah M. Levine, Jaclyn R. Wecht, Matthew T. Maher, James M. LiMonta, Sana Saeed, Tiffany M. Santiago, et al. 2020. "Posteroanterior Cervical Transcutaneous Spinal Stimulation Targets Ventral and Dorsal Nerve Roots." *Clinical Neurophysiology* 131 (2): 451–60. https://doi.org/10.1016/j.clinph.2019.11.056.

Yonemura, Hiroshi, Kazuo Kaneko, Toshihiko Taguchi, Hideaki Fujimoto, Kouichiro Toyoda, and Shinya Kawai. 2004. "Nerve Root Distribution of Deltoid and Biceps Brachii Muscle in Cervical Spondylotic Myelopathy: A Potential Risk Factor for Postoperative Shoulder Muscle Weakness after Posterior Decompression." *Journal of Orthopaedic Science* 9 (6): 540–44. https://doi.org/10.1007/s00776-004-0832-1.

Zehr, E. Paul, and Jacques Duysens. 2004. "Regulation of Arm and Leg Movement during Human Locomotion." *The Neuroscientist: A Review Journal Bringing Neurobiology, Neurology and Psychiatry* 10 (4): 347–61. https://doi.org/10.1177/1073858404264680.